Mechanical characteristics of Quenched and Self-Tempered (QST or TMT) steel reinforcing bars used in concrete structures

Sooraj A.O. Nair [a], Prabha Mohandoss [b], Kiran Ram [a], Tayyab Adnan [a], Radhakrishna G. Pillai [c,*]

[a] *Former Graduate Student, Department of Civil Engineering, Indian Institute of Technology Madras, Chennai 600 036, India*
[b] *Assistant Professor, Department of Civil Engineering, National Institute of Technology Tiruchirappalli, Trichy 620 015, India*
[c] *Associate Professor, Department of Civil Engineering, Indian Institute of Technology Madras, Chennai 600 036, India*

ARTICLE INFO

ABSTRACT

Quenched and Self-Tempered (QST) steel reinforcing bar (rebar herein) is widely used owing to its high strength and ductility over conventional hot-rolled or cold deformed bars. A typical QST rebar constitutes a composite microstructure of a hard 'tempered martensite' (TM) peripheral ring and a ductile 'ferrite-pearlite' (FP) core. TM and FP are predominantly responsible for the strength and ductility, respectively exhibited by a QST rebar. A good quality QST rebar cross-section shows a uniform, continuous, and concentric TM-ring around the FP core. However, recent studies reported that poor quality QST rebars with inadequate/defective cross-sections could influence mechanical and durability properties. This study evaluates the effects of inadequate cross-sectional phase distribution (CSPD) on the mechanical properties of QST rebars. In stage 1, tensile test on TM and FP extracted from a QST rebar clearly showed that FP is ductile with low strength, while TM had a brittle behaviour with high yield and ultimate strengths. In stage 2, the composite response of QST rebars collected from different manufactures were evaluated using tensile and bend tests to correlate the effect of CSPD. Tensile test results show a significant variability (up to 15%) in the stress–strain behavior and mechanical properties exhibited by rebars with inadequate CSPD while the failure pattern shows a composite response. Poor-quality rebar specimens in bend tests showed cracks which could induce crevice corrosion. Hence, CSPD has a significant influence on the mechanical and corrosion properties of a QST rebar. Acceptance criteria based on TM-ring percentage area and distribution in the CSPD is proposed to check the quality of the QST rebars.

1. Introduction

Tempered martensite (TM) steels have better tensile strength and hardness than conventional hot-rolled steel (mild steel) rebars. However, TM steels are brittle in nature while mild steel is relatively ductile. Quenched and Self-Tempered (QST) steel reinforcing bars ('rebar' herein), also termed Thermomechanically treated (TMT) steel rebars in the south-asian market, have a composite microstructure of a hard 'tempered martensite' (TM) peripheral ring around a ductile 'ferrite-pearlite' (FP) core. This is achieved through various patented cooling systems that rapidly 'quench' and 'temper' the hot rolled steel in the manufacturing line [1–3]. TM has higher yield strength but shows a brittle nature, whereas FP is relatively weaker but ductile in nature. The combined action of TM and FP are responsible for improved mechanical properties than its predecessors. Studies have compared the properties of QST rebars with other steels, in terms of strength, hardness, bendability, weldability, and corrosion resistance. A few studies reported the composite action of different microstructures, variation in tensile parameters, and geometrical characterization of QST rebars [4,5]. However, recent studies have observed inadequate cross-sectional phase distribution (CSPD) as a result of improper quenching [6] (see Fig. 1). The effects of this on the mechanical parameters of the QST rebars are not well-documented. To ensure the required strength and ductility, the thickness of TM ring should be adequate and uniform around the FP phase, referred as adequate CSPD herein (see Fig. 1) and the rebar is qualified as a good quality rebar herein.

Although QST rebars have been extensively used across the globe for more than three decades, the presence of inadequate CSPD has been

---

Abbreviations: QST, Quenched and Self-Tempered; TMT, Thermo Mechanically Treated; TM, Tempered Martensite; FP, Ferrite Pearlite; CSPD, Cross-Sectional Phase Distribution.
  * Corresponding author.
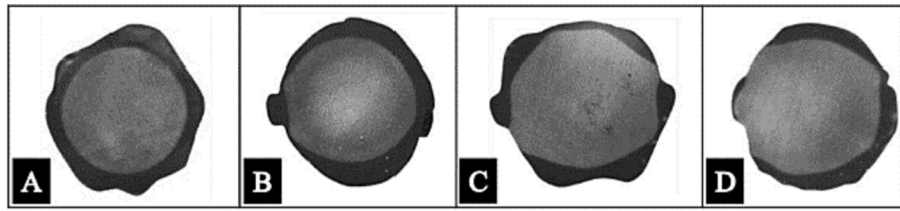   *E-mail address:* pillai@civil.iitm.ac.in (R.G. Pillai).

Fig. 1. Typical cross-sectional phase distribution (CSPD) of QST rebars showing (a) Continuous, concentric and uniform FP and TM phases (adequate) and (b-d) discontinuous, eccentric, or non-uniform phase distribution (published in [6]).

Table 1
Hardness of Tempered Martensite (TM) and Ferrite-Pearlite (FP) reported in literature.

References	Sample	Avg. Hardness (HV)	
		TM	FP
Rehm and Russwurm (1977) [10]	Heat 1	240	175
	Heat 2	250	165
Gamble (2003) [2]	Set 1	295	210
	Set 2	295	235
Nikolaou and Papadimitriou (2004) [9]	8 mm	310	225
	12 mm	300	200
Candoni et al. (2013) [7]	32 mm	275	165
	40 mm	290	185
Rocha et al. (2016) [5]	16 mm	270	155
	26 mm	275	155
	34 mm	280	175
Average		280	186
Std. Deviation		21	28
Coefficient of Variation		8	15

unnoticed and its implications have not been reported. The presence of inadequate CSPD could result in the variation of mechanical properties for a single rebar. This could lead to a shift in the design values of steel considered, say for under-reinforced design or strong column-weak beam design, and impact the reinforced concrete design calculations. The results from this study could quantify the variation in YTS to be accounted for, and to suitably adjust the factor of safety in design. Also, poor quality QST rebar used in stirrups under mechanical bending could form cracks and attract crevice corrosion. The discussion in this study is expected to build awareness on the need for good quality control and enhance quality in the manufacturing of QST rebars. Therefore, the present study evaluates the mechanical characteristics of QST rebars and its variability with respect to the CSPD of QST rebars, to suggest guidelines in assessing the quality of rebars towards better structural design and durability.

1.1. Effect of TM and FP on the composite mechanical behaviour of QST steel rebar

Very few researchers have attempted to examine the mechanical performance of QST rebars as a composite behavior of their microstructure. The tensile stress–strain response of TM and FP microstructures conforms to the expected theoretical behavior in terms of strength and ductility [7]. Several tests have been reported at high strain rates and the superimposed graphs reveal a composite performance similar to FP, indicative of a lack of TM contribution [7]. Since the tensile response of a QST rebar is a composite behavior, the failure pattern and fracture mechanics are expected to be an intermediate behavior between that of TM and FP. This is supported by the fracture patterns published elsewhere for as-received QST steel rebars and machined QST rebars [8]. Also, the yield tensile strength was similar for as-received and machined/milled rebars while the elongation at failure and ultimate strength values showed a marked difference [8]. Note that the composite performance can only be captured with the least disturbance over an as-received rebar condition when compared to machining recommended by conventional codal provisions. Specimen preparation is intended to define gauge lengths, control the failure region, and for other testing convenience. However, for a composite QST rebar, this could be detrimental to the peripheral TM-ring and bias the composite performance. The tensile response of as-received rebars can be closer to that of FP and the yield tensile strength had a marked difference as reported in [7]. An approximate calculation for E shows an underestimated value of 140 and 160 GPa for milled and as-received specimens, respectively, while an approximate E calculated is close to 200 GPa [7,8].
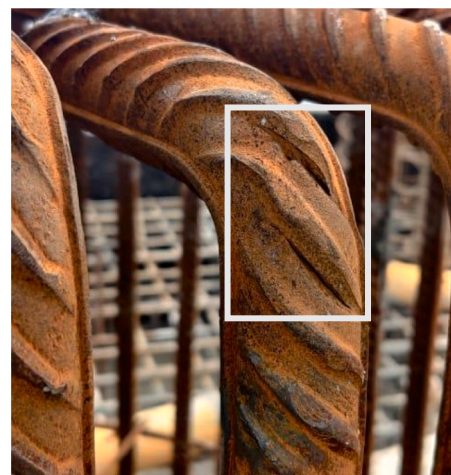
Fig. 2. (a) Photograph of the use of inappropriate mandrel at a construction site, and (b) cracks at the bending location of rebars.
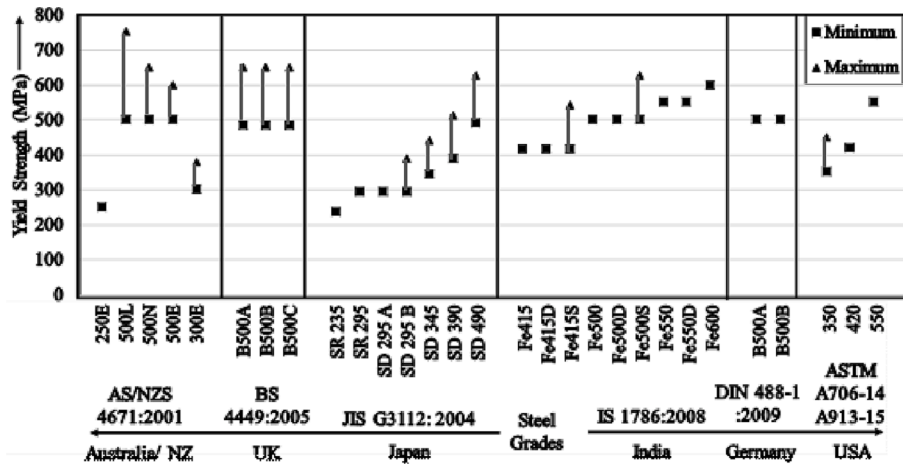
Fig. 3. Limits on yield tensile strength (YTS) available in different international standards.

1.2. Hardness, bendability and flexural stress concentrations in QST steel rebars

Studies have reported the variation in hardness across the diameter of QST rebars [5,7,9,10]. FP is softer than TM and the hardness profile across the rebar diameter will show higher values near the periphery and lower values at the core, and the reported values are given in Table 1. The hardness values range between 155 and 235 and 240–310 HV units (Vickers hardness scale) for FP and TM, respectively. QST rebars of 8, 10, 12, 16, and 32 mm diameter subject to bend tests exhibit good bendability and are formable without any visible cracks [10,11]. The position of specimens in bending (with transverse ribs or longitudinal ribs on the convex side of the bend) was not defined and the load–deflection behaviour has not been discussed in these studies. These might give a better understanding on the possible crack initiation and propagation mechanisms during in-situ bending. In addition, rib/surface profile can influence stress concentration and potential crack nucleation [5,12]. Surface imperfections from the manufacturing lines originate near the transversal and longitudinal ribs [5], and localized plastic deformation at the transverse rib root initiate cracks under fatigue cycles [12]. Because these imperfections are zones of stress concentration, these are potential failure zones in the service life of QST rebars under flexure. These observations could apply to the response on bending the bars, which could form localized stress locations and subsequent cracking. Mandrel diameter also plays a significant role while bending the rebar. Typically, the mandrel diameter should be three times the diameter of the rebar. Using a mandrel diameter lesser than or equal to the rebar diameter can develop visible cracks in critical sections mentioned earlier. Fig. 2 (a) shows a photograph of bending a rebar at the construction site using a mandrel of almost the same diameter of rebar. As a result, visible cracks were observed at the bending location as shown in Fig. 2 (b). Such cracks are critical and could significantly influence the mechanical and durability properties of QST bars.

1.3. Comparison of international codes for tensile performance of steel rebars

The international codes for the quality control of steel rebars for concrete does not mandate the method of manufacturing. Basu et al. (2004) [13] has compared several international standards on mechanical properties for similar grades of rebars. All the codes require minimum tensile parameters for the manufactured steel rebars, which include yield tensile strength (YTS), ultimate tensile strength (UTS), UTS/YTS ratio, and percent elongation. However, the availability of different grades of steel and the closeness in their properties may result in compromising the quality of steel rebars in terms of the expected

values. For example, an Fe 550D rebar could pass the specifications for an Fe 500D rebar also. This is because the qualification requirements are based on minimum limits. However, a clear demarcation with maximum limits to distinguish between different grades are not present in most of the international codes of practice. Fig. 3 illustrates the minimum and maximum limits of YTS across NZ, JS, BS, BIS, and ASTM codes [14–22]. The YTS is a crucial factor in the design of reinforced concrete structures and needs to be controlled within stipulated limits [14–22]. Typically, as per the specification, an Fe 500D bar might not exactly have 500 MPa as the YTS (or within 550 MPa) and the expected YTS is open-ended for any value above 500 MPa. Comparing this case with an Fe 500S bar, which has an upper limit of 625 MPa, a design for an under-reinforced concrete element or for a seismic prone building could anticipate the maximum possible yield strength in-situ for the given rebar grade [20].

Most of the steel grades in the International codes (DIN and ASTM standards) do not put upper limits on the YTS. While the upper limit on YTS is specified for Fe 415S and Fe 500S rebar in IS 1786:2008 and 13920:2014, the same is not mentioned for the other classes of rebar. The mechanical parameters should meet these codal provisions irrespective of the technology by which a rebar is manufactured. However, an additional advantage of providing upper limits on YTS will be an indirect control over the quenching and optimized parameters to achieve a good quality QST rebar in its microstructural requirements explained in the later sections. Unlike YTS, this issue is not profound for other parameters like UTS or % elongation, since higher values are advantageous in these cases. Note that the effect of an inadequate CSPD is still not well-documented and the results from this study could help explain the tensile and flexural observations in rebars with inadequate CSPD. However, hardness of rebars need not be checked in the case of inadequate CSPD, since the underlying fact that FP is softer than TM is applicable in both the cases of cross-sectional adequacy (adequate and inadequate CSPD).

2. Materials and methods

This study was executed in 3 stages viz. (1) Mechanical properties of isolated and composite microstructures, (2) Mechanical properties of composite microstructures of 10 sets of steel rebars from different manufactures and (3) Bending induced crack resistance of QST rebars. The scope includes tensile and flexural properties evaluated by tension tests and bend tests, respectively. QST rebars of 500D grade with 8, 12, and 16 mm diameters were used for the tests. The specimen preparation for tensile and bend tests are detailed as follows.
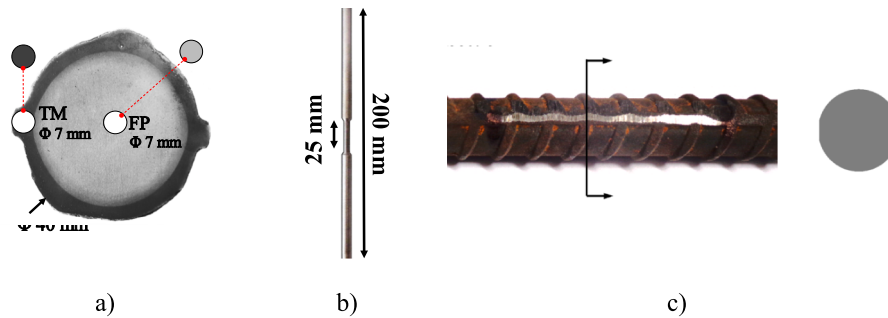
Fig. 4. (a) Test specimen etched and showing locations of TM and FP specimens extracted, (b) typical test specimen extracted for tensile test with dimensions, and (c) longitudinal rib milled in tensile test specimen preparation of full rebar.

2.1. Comparison of tensile test behaviour of FP, TM, and QST rebar specimens

The mechanical behavior using tension tests was evaluated in two different types of specimens.

(i) Type 1 (Isolated microstructure): TM-alone and FP-alone specimens were extracted from a 40 mm diameter rebar as shown in Fig. 4 (a). The extracted cylindrical specimens were 200 mm long. TM specimen was extracted by Electron Discharge Wire (EDW) cutting and subsequent machining for specimen preparation (see Fig. 4 (b)).

(ii) Type 2 (Composite microstructure): As-received specimens from good and poor quality steel rebars were tested in this case. The specimens were prepared by milling the longitudinal ribs/ seam alone in the gauge length (GL) to anticipate the failure in the region of reduced cross-section. The length of milling was 5 times the diameter as per the gauge length requirements specified by IS 1786: 2008 [19].

Tension tests were done on FP, TM, and a QST rebar specimens to compare the yield tensile strength (YTS), ultimate tensile strength (UTS), percent elongation (δ), YTS/UTS ratio, and Young's modulus (E). This was followed by as-received QST rebars with good and poor quality CSPDs subjected to tension test for comparing the tensile performance. As-received tensile test specimens were not milled on a lathe to reduce the cross-section as per the codal provisions. This is because the TM ring will be disturbed/removed, giving an underestimated test result when compared to as received bars. This is generally the case when strain is measured for a specific GL which requires milling. In industry, the technician puts marks (using a marker or dot punch) at equal intervals along the specimen length and tests the specimen. The elongation percentage is calculated for the interval in which the specimen breaks. However, a better means of preparing the GL is used as shown in Fig. 4 (c). The longitudinal rib/seam is milled or ground to make the effective area relatively lesser than the other areas, retaining the TM ring undisturbed to ensure that a composite response is achieved under the tensile testing.

The tension test parameters were based on the standards of practice (IS 1608: 2005 and ASTM E8: 2008) and user requirements. Specimens in this study were tested in an MTS 311.12 universal testing machine (UTM) with an HBM QuantumX MX 1310-B data acquisition system to record the strains measured by an indigenously fabricated extensometer. For the specimens of Type 1 (isolated microstructure), the tensile test was done for a specimen diameter of 5 mm in a GL of 25 mm (5 times the diameter in test region). The specimen length was 200 mm and the gap length (specimen length minus grip length) after setting the specimen on UTM was 90 mm. The loading rate was 1.25 mm/s [17]. Similarly, for specimens of Type 2 (composite microstructure) the tensile test was done with a specimen diameter of 10 and 12 mm. The length of milling was 5 times the diameter as per the gauge length requirements specified by IS 1786: 2008 [19].

2.2. Capturing CSPD of QST rebars using TM-ring test

Fig. 5 shows the expected CSPD observed after TM ring test used as a qualitative benchmark for good quality rebars. This CSPD of the QST rebars was captured using TM ring test with the setup shown in Fig. 6. The specimen preparation for TM-ring test involves rebars being cut, embedded in an epoxy, and polishing the transverse cross-sectional surface of the embedded rebar in epoxy [6]. Since the steel microstructure is sensitive to temperature, care was taken while cutting and
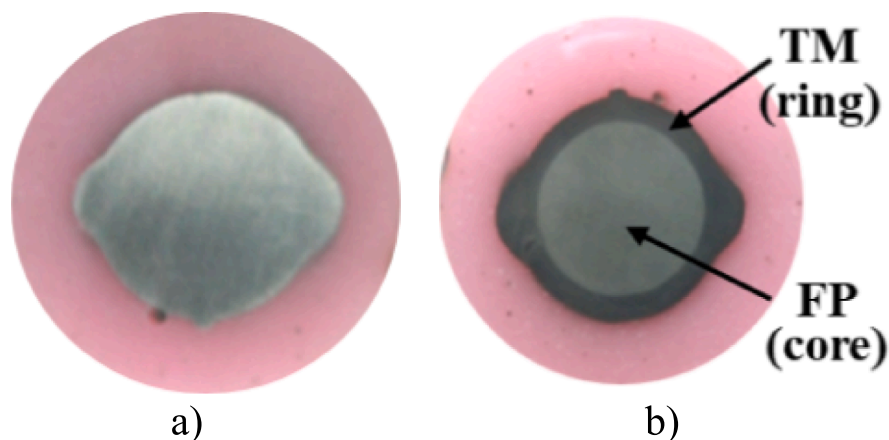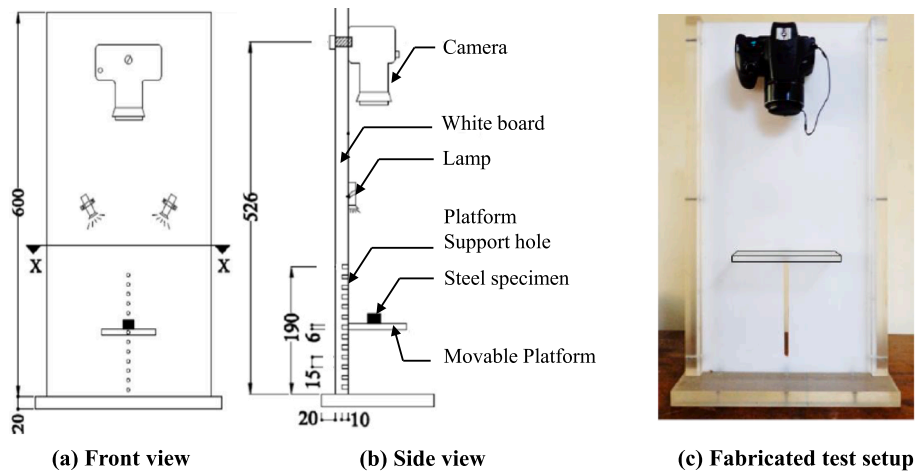

Fig. 5. TM-Ring test specimen showing (a) specimen embedded in epoxy before testing, and (b) specimen after testing with the expected/adequate CSPD for good quality bars (concentric FP inside uniformly thick TM-ring).

(a) Front view   **(b) Side view**   **(c) Fabricated test setup**

Note: All dimensions are in mm

Fig. 6. Cross-section phase distribution (CSPD) imaging using TM-ring test showing different schematic views and overall test setup.

Before testing   After testing

(a) Schematic of the setup   **(b) Real time setup**
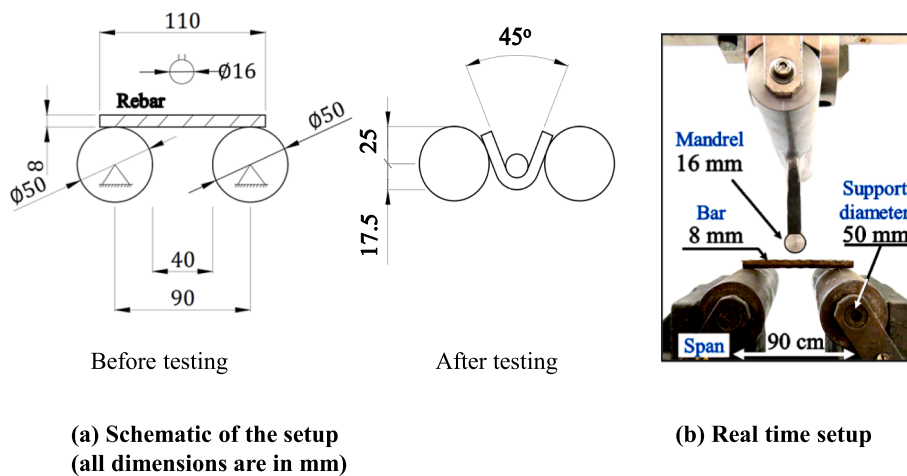**(all dimensions are in mm)**

Fig. 7. Bend test setup showing (a) schematic of the setup before and after testing with the dimensions marked, and (b) snapshot from the actual test setup with a rebar in place.

preparing specimens for the test. Therefore, based on the recommendations given in [6], steel rebars were cut using a handsaw or an abrasive cutter with continuous supply of coolant. The use of coolant helps to limit the temperature of steel, which will avoid any transition or changes in TM and FP phases. The sharp edges of cut rebars were smoothened by using silicon carbide abrasive sheets, while a metal polishing machine was used to achieve effective smoothening. The smoothened steel specimen was molded in translucent/opaque cold setting epoxy with good surface finish. The setting time of epoxy was typically about 10–15 min and the silicone rubber moulds were used to remove the molded specimens easily. Care was taken to avoid air bubbles getting trapped in the epoxy while mixing/placing the epoxy. The molded specimen surface was coarse polished using abrasive sheets of 80, 150, 220, 320, and 600 grit sizes in sequence. It is important to avoid rise in the temperature of steel specimens by supplying water or coolant continuously to absorb the heat generated while polishing. Specimens were macro etched using Nital (5 % Nitric acid in alcohol) to capture the CSPD. The sequence of steps to obtain the CSPD using the setup shown in Fig. 6 includes 1) mounting the camera in position, 2) placing the specimen on the movable platform (stage), 3) adjusting the height of the specimen stage, 4) measuring the light intensity, and 5) placing a ruler and capturing the image for post processing. A detailed 'TM-ring test' procedure is published in a companion study [6].

It is easy to extract an isolated FP specimen from a QST rebar by milling the outer layer to the required depth (see Fig. 4 (a)). However, isolating a cylindrical TM specimen is difficult and needs proper supervision. A 36 mm diameter and 200 mm long QST rebar's cross-section was macro-etched to identify the thickness of TM and the available thickness was relatively near the longitudinal rib area (shown in Fig. 4 (a)). Based on this, the specimen diameter was decided as 7 mm, and was cut and milled out of the rebar edge to isolate TM. The 200 mm long specimen was milled further to a diameter of 5 mm at the center for a 25 mm length as the GL. The specimen was etched using 5 % nitric acid in ethanol to confirm that the GL does not have isolated spots of FP present.

2.3. Bending-induced crack resistance of QST steel rebars

Bend tests were executed in rebars of 8 mm diameter as shown in Fig. 7. Rebars from 10 different manufacturing sources were tested, which includes 2 sources with adequate CSPD and 8 sources with inadequate CSPD. The bend test was also divided into two cases.

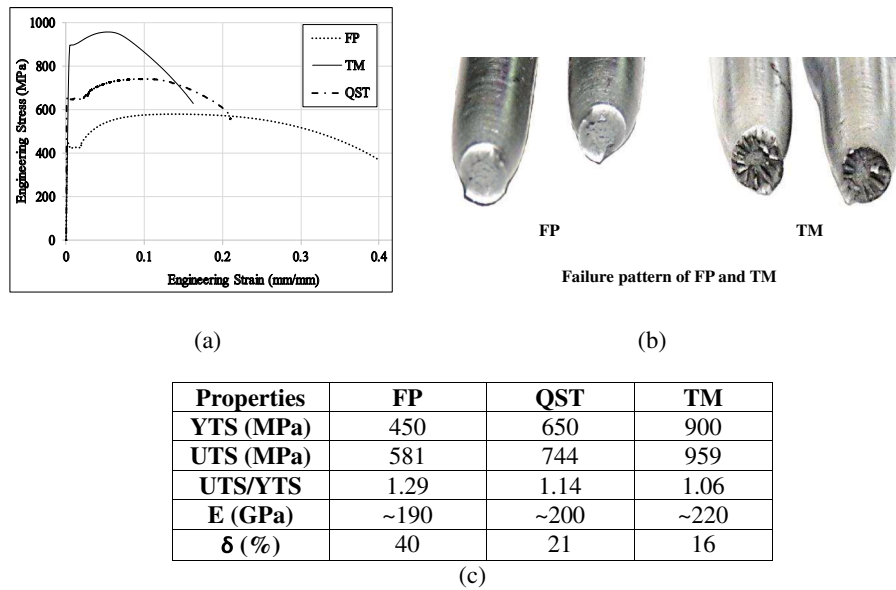(i) Case 1: A standard 135° bend test (included angle 45°) as per IS 1599:2012 [23].

(a)

FP   **TM**

Failure pattern of FP and TM

(b)

Properties	FP	QST	TM
YTS (MPa)	450	650	900
UTS (MPa)	581	744	959
UTS/YTS	1.29	1.14	1.06
E (GPa)	~190	~200	~220
δ (%)	40	21	16

(c)

Fig. 8. Tensile test results of isolated microstructures showing (a) Stress–strain behaviour of FP, TM, and QST steel rebars, (b) failure surfaces observed, and (c) observed test results on strength, stiffness, and ductility.

(ii) Case 2: A modified bend test for a bend angle of 157.5° (included angle of 22.5°) intended to simulate excess bending.

IS 1599: 2012 specifies a mandrel diameter between 2 and 20 times the diameter 'd' of the rebar tested. The mandrel diameter used was 16 mm to mimic a site scenario of an 8 mm stirrup rebar, bent around a 16 mm primary rebar. The bars were checked for visible cracks on the convex bent surface at bend angles of 45° and 22.5°.

An improvised bend test setup from the codal provisions in IS 1599: 2012 was used as shown in Fig. 7 (a) and (b). The loading rate was 1 mm/s of the centre deflection and continued until a target displacement of 42.5 mm was achieved. This displacement corresponds to a bend angle of 135° (included angle of 45°) for the current setup (after testing shown in Fig. 7 (b); 25 + 17.5 = 42.5 mm). The mandrel diameter was 16 mm, and the rebars were bent across a test span of 90 mm and a clear span of 40 mm. The minimum clear span should be equal to the diameter of mandrel plus 3 times the diameter of rebar (40 mm in this case) as per the codal provision. The support hinges had a diameter of 50 mm. The orientation of the bar will affect the response in the bend test. i.e. if a specimen is placed with its longitudinal rib at the bottom, the possibility of crack formation might be less. However, in the case of a good quality QST rebar, this might not make a difference. The rebars were consistently placed such that the longitudinal ribs are perpendicular to the

loading direction.

3. Results and discussion

3.1. Isolated vs Composite microstructure

3.1.1. Stress–strain behaviour and failure patterns

The stress–strain behaviour of the extracted FP and TM specimens is shown in Fig. 8. The characteristic values are also shown along with the graphs. It is clear that FP is more ductile (60 % higher) than TM. However, FP has a 50 % lower yield strength (about ~ 450 MPa) than TM (about ~ 900 MPa). E-values for both specimens were about ~ 200 GPa. The UTS/YTS ratio for TM was lower than FP. The plateau near ultimate stress is relatively longer for FP, which shows its ductile nature. This is reflected in a final elongation of 40 % for FP when compared to 16 % for TM (almost 2.5 times). The response of a QST rebar (composite rebar; dashed-dotted line) showed an intermediate behaviour between FP and TM. The lack of ductility in TM and lack of strength for FP were compensated by each other (Note: strength in general represents both yield and ultimate strength). This is evident by an intermediate ductility and strength values as observed in the stress vs strain plot (Fig. 8(a)). The composite behaviour showed an increase of about 50 % in the YTS from FP and 30 % in the final elongation from TM. The YTS_{QST} evaluated
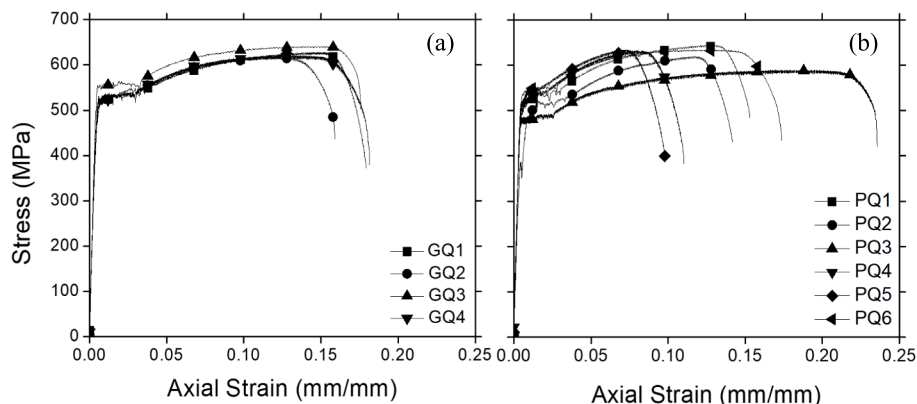

Fig. 9. Tensile stress–strain relationship of (a) good quality (showing relatively lower variability) and (b) poor quality rebars (showing higher variability).
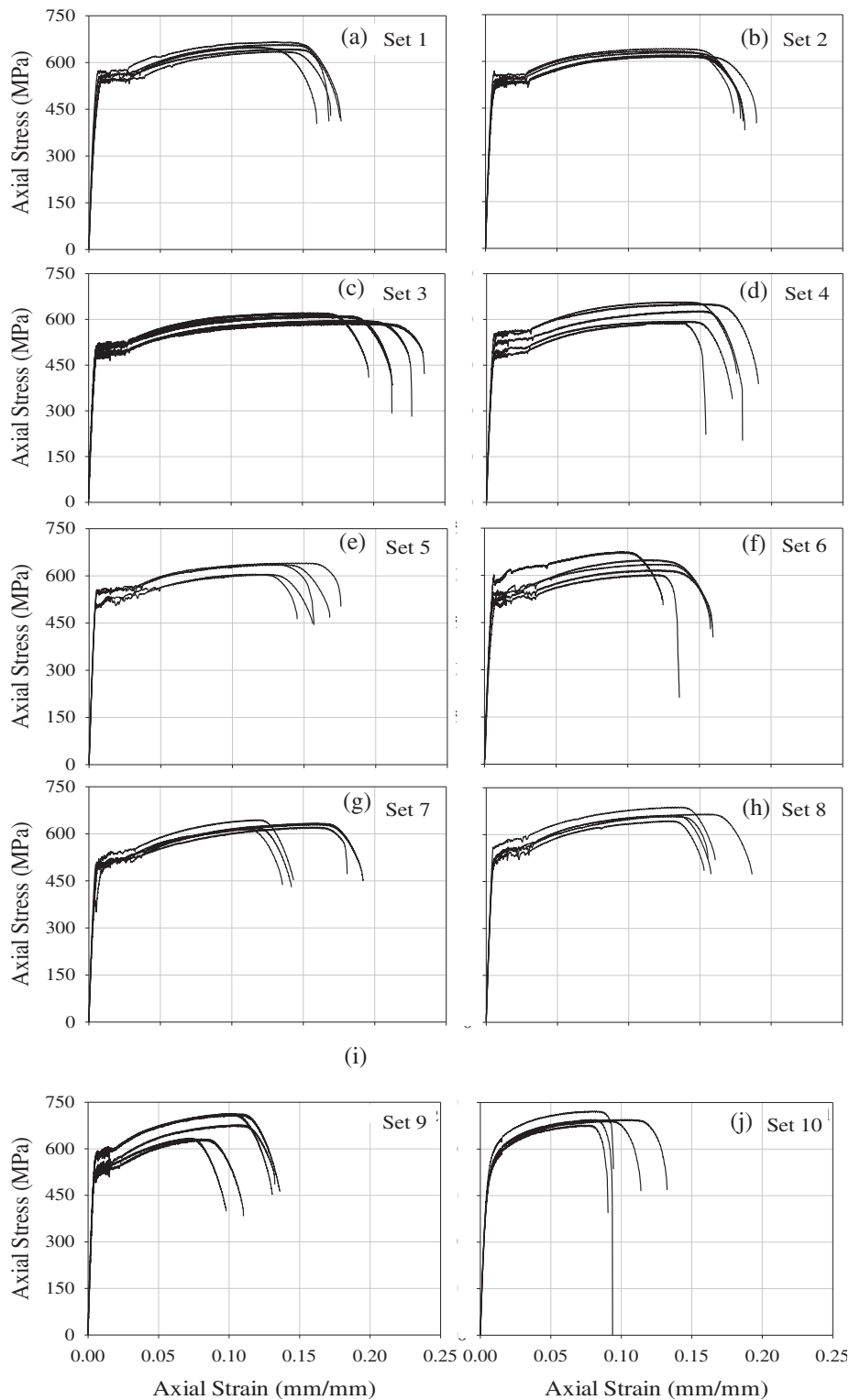
Fig. 10. Tensile stress–strain relationship of QST rebars for several sets of rebars from various manufacturers.

was approximately equal to the average of YTS$_{FP}$ and YTS$_{TM}$ assessed, showing a strong correlation of a composite behavior of the multiple microstructures. The results confirm that the strength characteristics of a QST rebar is predominantly given by TM, whereas the ductility is given by FP (Fig. 8(b) and (c)).

The failure patterns closely agree to the theoretical formation as shown in Fig. 8 wherein FP showed a nearly ductile failure, with a 'cup and cone' failure surface. However, the end shear due to the sudden energy release at failure causes a slip plane to form. Otherwise, the failure pattern of FP clearly resembles that of a typical ductile material. For TM, although a slight neck has occurred, the failure was by predominant shear with shear planes visible as sharp corrugations. The failure plane was not flat as in a typical brittle failure. However, multiple shear planes that slipped and ruptured are visible on the failed surface.

Table 2
Mechanical properties of rebars from different manufacturers.

Source ID	YTS in MPa {CoV in %}	UTS in MPa {CoV in %}	δ in % {CoV in %}	UTS/YTS
Set 1	540 {3}	651 {2}	18 {03}	1.20
Set 2	520 {2}	629 {2}	17 {04}	1.18
Set 3	515 {7}	624 {5}	15 {11}	1.21
Set 4	503 {2}	607 {2}	22 {07}	1.21
Set 5	535 {6}	636 {4}	17 {08}	1.19
Set 6	516 {2}	652 {3}	16 {07}	1.26
Set 7	540 {3}	674 {6}	12 {14}	1.23
Set 8	565 {3}	696 {2}	11 {14}	1.26
Set 9	510 {2}	664 {2}	16 {08}	1.25
Set 10	523 {2}	627 {2}	15 {16}	1.48

3.1.2. Variation in tensile parameters of good and poor-quality steel rebars

Fig. 9 (a) and (b) shows the stress–strain graphs for a set of 4 - good quality (GQ) and 6 - poor-quality (PQ) steel rebars tested under tension, respectively. It was observed that the lower limits of tensile parameters as specified in the codal provisions were met by both sets. However, a relatively higher scatter is observed in the case of poor-quality steel rebars. This scatter is caused by the difference in stress–strain behavior of FP and TM in low-quality rebars and inadequate CSPD. Therefore, it is important to determine the CSPD in conjunction with the tensile tests to check the quality of rebar in terms of its stress–strain behavior. For this purpose, 10 sets of rebars from different manufactures were collected and tested, and the results are discussed in the following section. Note that both sets of rebars exceed the upper limit of yield strength (600 MPa) given in the amended draft of IS 13920: 2014. Also, the required UTS/YTS value of 1.25 is not met by a few sets, which makes them inadequate as per BIS standards for their use in seismic zones. This adds to the need for controlling the CSPD for better and consistent quality for steel rebars for design considerations.

3.1.3. Stress–strain behavior of QST rebars with different CSPD

Fig. 10 shows the stress–strain behavior and Table 2 shows the mechanical properties of QST rebars from different manufacturers. Depending on the CSPD of the rebars, stress–strain behaviour of QST rebars was provided, representing the CSPD ranging from good to poor state. Among these 10 sets of rebars, Set 1 and Set 2 exhibit uniform stress–strain behavior while others show notable variability. Set 9 and Set 10 exhibit poor performance, especially Set 10, which does not have a definite yield point as expected in QST rebars.

The CSPD of rebars is responsible for the expected stress–strain behavior of QST bars from different manufacturers. In order to understand the mechanical behavior with respect to CSPD, the CSPD of one representative rebar from each set is captured and related to their stress–strain behavior as shown in Fig. 10. A good quality rebar containing two phases (FP and TM; see Section 2, Fig. 5) with uniform TM ring results in nominally invariant (CoV < 3) stress–strain behavior of QST rebars, exhibited by Sets 1 to 3 (See Fig. 11 (a - c)). The TM-ring of Sets 4 and 5 is uniform with locally concentrated FP exclusion (or an eccentric core) where the thickness is slightly less than other regions. This variation in TM ring thickness resulted in higher scatter in the ductility of rebars (as observed in Fig. 11 (d) and (e)). Higher thickness of TM ring might cause brittle failure in the structure [8]. The rebars from Set 6 exhibited uniform thickness of about 90 %, although an incomplete ring is observed with a local absence of TM region, which significantly affected the ductility of rebar as shown in Fig. 11 (f) (see Set 6). Fig. 11 (g) and (h), Set 7 and Set 8 have a discontinuous TM ring along the periphery, which exhibited a significant influence on both the strength as well as the ductility.

Set 9 and Set 10 have very inconsistent outer TM ring (See, Table 2 which indicates high CoV)shown in Fig. 11 (i) and (j). Although these sets have lesser TM and more FP, their behaviors conflict with the expected mechanism of a typical QST rebar. It is expected that the strength

should be relatively lower since the area of TM is lower, and ductility should be relatively higher since the area of FP is higher. However, both these sets exhibited high strength and less ductility, and failed in brittle mode. This could be due to the poor practice in the rolling process and quality control from respective manufacturers [24]. It is to be noted that poor manufacturing practices could result in such scatter in CSPD, which influence the CSPD along the length of the same rebar [25]. This could be one of the reasons why the CSPD of Set 9 and 10 and their behaviour did not match consistently with the results of other sets of rebars.

CSPD is highly influenced by the manufacturing process due to many influencing factors such as rolling speed, composition, and heating and cooling rates [26]. For instance, if the cooling rate is not synchronized adequately, it significantly affects the TM ring performance. Therefore, a poor CSPD indicates that the manufacturing process was not done properly, and hence the quality is not satisfactory to accept such rebars for structural applications. The significance of such poor CSPD is given below:

(1) Hardened periphery above 30 % of the total cross-sectional area represents highly over-quenched bars which results in high yield strength and poor ductility.

(2) Non-uniform hard periphery indicates that the quenching has not taken place uniformly around the periphery. Such bars should be used only after extensive testing and evaluating the scatter in the results.

Many reinforced concrete design codes (including *ACI* 314, 2014 and *fib*-MC 10) suggest that yield strength and ultimate strength of steel rebars should not be significantly higher than the assumed design values. If the upper limit exceeds the design values significantly, then the steel reinforced concrete section would not perform as under-reinforced as expected. If the yield strength is greater than the assumed design strength, it could cause undesirable failure mode like brittle failure instead of required ductile failure. This condition is critical, especially in seismic zones, where ductile mode of failure is desirable for a safe design. On the other hand, if the yield strength is lower than the design value as in the case of non-standard rebars, margin of safety would be reduced, thus resulting in an increased risk of premature failure. This sensitizes the importance of taking care of the upper limit of the yield strength.

IS 1786 (2008) suggests a minimum elongation of about 12 % and 16 % for Fe500 and Fe500D, respectively. The UTS/YTS ratio for 500 and 550D should be greater than 1.08 and 1.10, respectively, where UTS should not be<545 and 565 MPa for Fe500 and Fe550D, respectively. Table 2 shows the mechanical properties of rebars from different sources of manufacturers. Rebars from these sets (Sets 1 – 4, 7, and 8) represent Fe550D and Sets 5, 6, 9, and 10 represent Fe500. The tested rebars satisfy the lower limit of YTS and UTS, but certain sets (Sets 3, 7, and 8) failed to meet the required elongation as specified by IS 1786 (2008). Also, many of the rebars from different sets did not meet the UTS/YTS ratio of 1.25 as required by the codal provisions. These results emphasize the need for a standard quality control test to avoid using poor quality rebars in construction.

3.2. 'Bending-crack' resistance

The rebars tested in tension behavior were of 12 mm diameter. However, the variation would be profound in 8 mm diameter rebars since they undergo the least quality control in the manufacturing line. Since 8 mm rebars are not used as primary reinforcement, the variability in tensile properties might not be an issue in the primary design calculations. However, these are used in design of stirrups and might pose an issue by exhibiting significant scatter in tensile behaviour, especially in seismic applications. Therefore, 8 mm rebars used in stirrups and hooks are critical for achieving the desired service life. Hence, good and poor quality QST steel rebars of 8 mm diameter were selected for bend test.
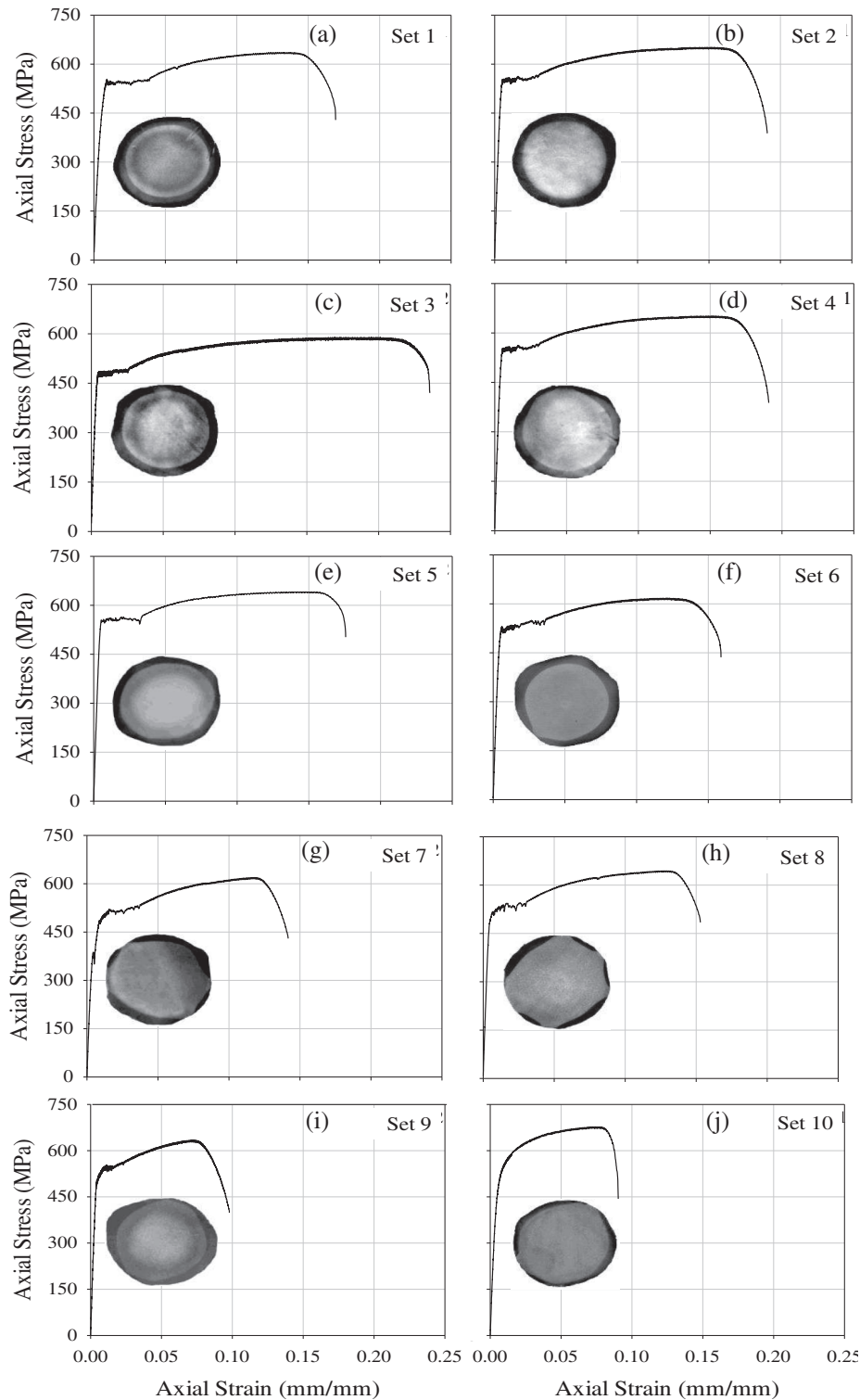
Fig. 11. Representative tensile stress–strain behaviour of QST rebars from each set (Fig. 10) with their respective CSPD.

3.2.1. Load versus deflection graphs

The superimposed load-bent angle graphs for bending up to 135° are given in Fig. 12. It is evident that the scatter in the peak loads and overall test response is higher for poor quality steel rebars. Although the number of good quality steels tested are less (owing to the lack of good CSPD in 8 mm bars available), the scatter seems to be higher in poor quality rebars in terms of the angle at peak load. Poor CSPD is predominantly seen in 8 and 12 mm rebars where the smaller bar diameter requires better quenching methods to get a uniform TM ring [6]. A maximum

scatter of 0.5 kN (<10 % of average peak load) is observed in the pre-peak and peak loads reported for good quality rebars while it is about 2.5 kN (≈ 45 % of the average peak load) for the poor quality rebars. Hence, the scatter could also be used as an indirect means of identifying inadequate CSPD.

3.2.2. Crack formation in poor quality vs Good quality QST steel rebar

All the rebars qualified the test for 45° (or 135° bend, as per IS 1786:2008 and IS 13920:2014). However, there were visible cracks in
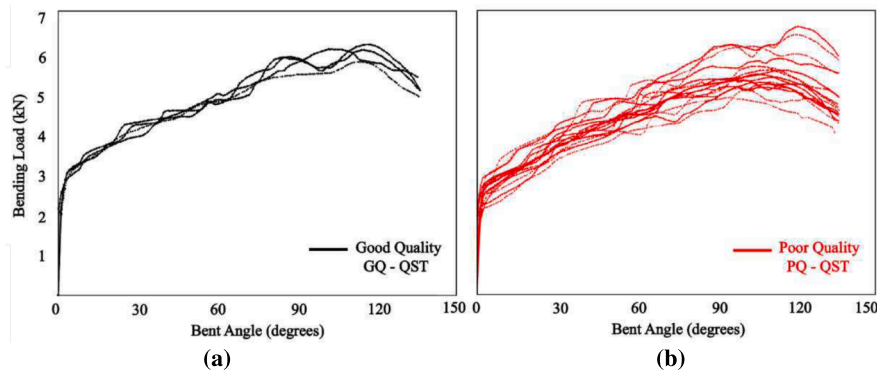
Fig. 12. Bend test response showing the bending load versus bending angle behaviour of (a) good quality, and (b) poor quality rebars.
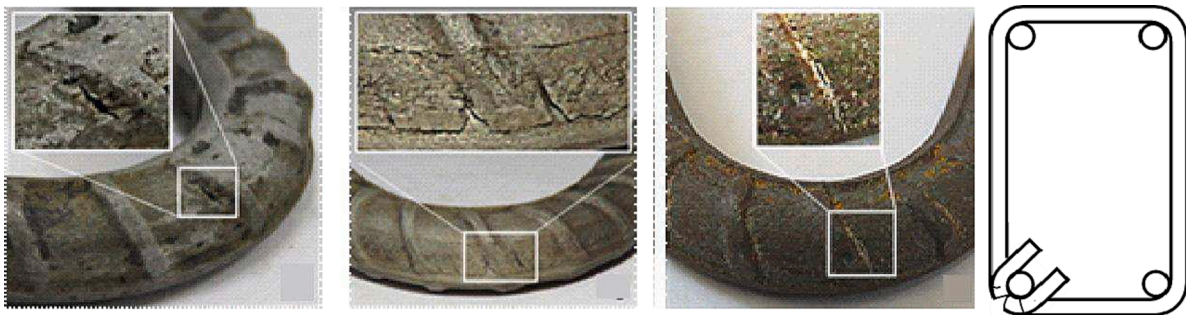

Fig. 13. Critical failure conditions showing (a-c) Cracks formed during bend test, and (b) schematic showing the potential location in real-time stirrups under excess bending.
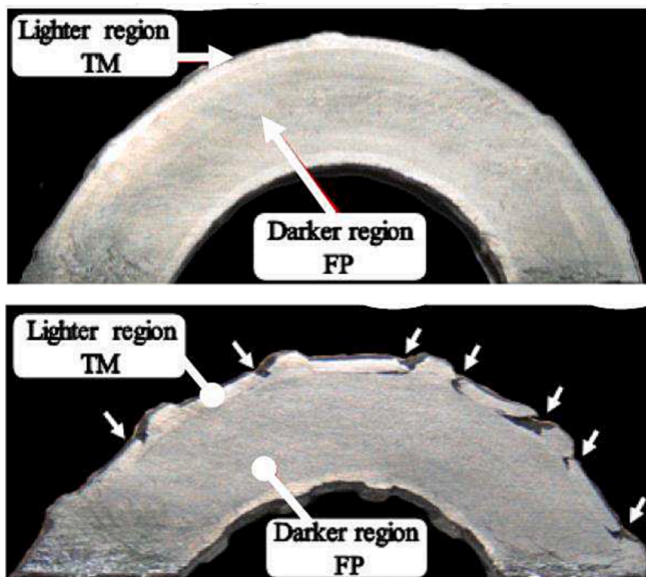

Fig. 14. Milled section of post-bent QST rebar specimens showing (a) a good quality rebar with continuous and uncracked CSPD, and (b) a poor quality rebar showing cracks at the surface.

transverse (tensile cracks) and longitudinal direction by bending to an included angle of approximately 22.5° (i.e. 22.5° bending). The frequency of cracking is less in terms of 'visible cracks' for poor quality rebars on 22.5° bending. Among the 8 sources of poor-quality steel rebars tested (shown in Fig. 12), 3 sources showed cracks under bending. However, since the bent angle is only 157.5°, it is expected to observe cracks in rebars with close bends (180°) used in hooks. Also, the in-situ

practices might not follow an exact bend angle of 135° for stirrups in seismic zones.

A few cases of cracks observed during the bend test are shown in Fig. 13 (a-c). These cracks are formed at the outer surface of the steel, which is near the concrete surface (schematic shown in Fig. 13 (d)),and will be a governing factor for crevice corrosion initiation [27–28]. Hence, the quality of steel rebars in stirrups with 22.5° bending (or higher) is crucial for structures in seismic zones. Several poor quality rebars showed stretch marks on the convex bent surface at 22.5° bending which were not considered as visible cracks. However, the rebars would have started forming cracks at this angle and are located mostly near the rib roots. These comply with the observations made in literature on stress-concentrations near the rib roots. A few other specimens showed mill scales opening up which were also not considered as crack openings.

3.2.3. Mechanism of cracking in poor quality QST steel rebars

Specimens from good and poor quality QST rebars were analyzed for CSPD in the bent region after the bend test. This was done by milling the bent bar to a depth (from the surface), where the crack-ends were visible. The images of the macro-etched bent surface are given in Fig. 14. It is evident that a good quality QST steel rebar has a perfect TM-ring and the bending stress at the extreme fibers are taken care of by the hard-tempered martensite (Fig. 14 (a)). However, in a poor-quality rebar, the specimen with severe cracking (both transverse and longitudinal) showed multiple locations of crack formation visible on the milled plane (Fig. 14 (b)). It is noticed that the transverse cracks propagate in the longitudinal direction along the TM-FP interface. The delamination of TM over FP is attributed to the FP-TM interfacial strain incompatibility at high loads. The milling should ideally be done till the center of the crack length (crack nucleation point in the interface), where it would have originated. At this location, there is a probability of finding an FP phase. This defective CSPD will attract cracks at the locations of FP appearing at the extreme fibers. This is because FP has only 50 % of the
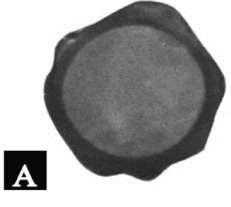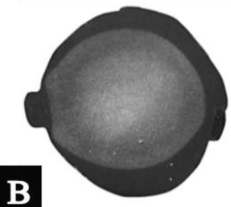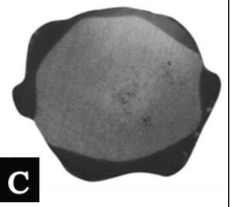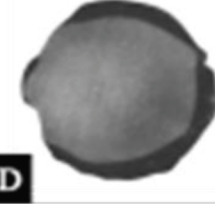
| table below |
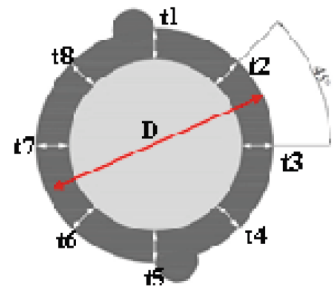
Data sheet for TM ring test

Reference cases

CSPD	A	B	C	D
	Acceptable	Not acceptable	Not acceptable	Not acceptable

Q. No.	Question				Answer
1.	1 Is a dark grey peripheral region and light grey core seen?				Yes / No
2.	2 Does the dark grey peripheral region form a continuous outer ring?				Yes / No
3.	3 Diameter of the rebar, D (mm)				

4.	1	t_1		t_5	
		t_2		t_6	
		t_3		t_7	
		t_4		t_8	
		Average measured thickness of TM ring, t_{TM} (Refer figure)			

5.	2 Average measured thickness of TM ring, t_{TM}

Nominal diameter (mm)	4	5	6	8	10	12	16	20	25	28	32	36	40
t_{min}[a]	0.3	0.4	0.4	0.6	0.7	0.9	1.2	1.5	1.8	2.1	2.4	2.6	2.9
t_{max}[b]	0.4	0.5	0.6	0.8	1.1	1.3	1.7	2.1	2.6	2.9	3.4	3.8	4.2
t_{avg}[c]	0.4	0.4	0.5	0.7	0.9	1.1	1.4	1.8	2.2	2.5	2.9	3.2	3.6

[a] Minimum allowable thickness of TM (considering the entire periphery, and not only the 8 measured values), $t_{min} = 0.07 D$

[b] Maximum allowable thickness of TM (considering the entire periphery, and not only the 8 measured values), $t_{max} = 0.10 D$

[c] Average measured thickness of TM ring (considering eight set of values along TM phase), $t_{avg} = 0.85D$

Fig. 15. Datasheet for acceptance criteria to qualify rebars based on cross-sectional phase distribution (CSPD).

YTS compared to TM. Once the crack starts, it propagates along the rib root/boundary. Once a crack forms, the failure could focus and stresses concentrate at the initiated point. However, there are more than one crack-initiation points in extreme bending scenarios as in the current case.

3.3. Acceptance criteria for TM - ring

Based on the experimental results, the CSPD of poor quality rebars can be classified as one of the following types:

1. Eccentric and non-uniform TM phases
2. Discontinuous and non-uniform TM phase

In addition to this, bending cracks occur when the poor quality rebars are used as stirrups. Therefore, acceptance criteria were proposed to qualify the rebars as part of associated literature [6,16]. Fig. 15 shows the data sheet for acceptance criteria to qualify the QST rebars, based on visual analysis (Q. No. 1 & 2) of CSPD. This qualification depends on the color to identify the inner and outer region and uniformity of phase distribution. Then, geometrical analysis (Q. No. 3 to 5) by measuring the diameter and thickness at 45° angle of rebars is suggested to check the uniformity.

The quantified results are compared with the minimum and maximum allowable thickness of TM for meeting the required strength and ductility of the rebars. The average measured thickness of the TM ring at 45° angle along the TM phase periphery (i.e., eight sets of values) should be between 0.07D and 0.1D as the minimum and maximum allowable thickness [6,16]. Note that literature recommends an area of TM-ring between 25 and 53 % of the overall cross-sectional area to achieve the required composite performance of QST steel rebars. This was used to back-calculate the recommended average thickness of the TM ring as mentioned above. Hence, to qualify a QST rebar as adequate,

the specimen should pass both visual and geometrical analyses. If it fails to meet any one of these analyses, then that batch of specimens should be rejected.

4. Conclusions

In this work, mechanical characterization studies of QST rebars including (a) assessing the effect of inadequate CSPD on the tensile parameters, and b) assessing the crack resistance of rebars under bending, were elaborated. The conclusions drawn from this study are as follows.

(1) The tensile behaviour of FP and TM closely follows a purely ductile and brittle material, respectively. Hence, the combined action of these phases contributes to the composite tensile response of QST steel rebars. The composite behaviour showed an increase of about 50 % in the YTS from FP-only and 30 % in the final elongation from TM-only response.

(3) QST steel rebars with inadequate and relatively high variability in CSPD along the length of the rebars can result in non-uniform stress–strain behaviour and significant scatter in yield strength. The tested rebars with good and poor quality CSPD did not meet the BIS standards for use in under-reinforced design and seismic zones. This emphasizes the need for controlling the CSPD for better and consistent quality for steel rebars in design considerations.

(4) The CSPD of rebars is responsible for the expected stress–strain behavior of QST rebars. Only 3 among 10 sets of rebars showed good quality with a uniformly thick peripheral TM ring, which exhibited the recommended stress–strain behavior among 10 different manufacturers. The tested rebars satisfy the lower limit of YTS and UTS, but several sets failed to meet the required elongation and UTS/YTS ratio specified by IS 1786 (2008) and IS 13,920 (2014) respectively. These results emphasize the need for a standard quality control test to identify poor quality rebars in construction.

(5) Load-deflection behaviour during the bend test showed relatively higher scatter for rebars with inadequate CSPD. Poor CSPD is predominantly observed in 8 and 12 mm rebars which requires better quenching methods to get a uniform TM-ring. Also, inadequate CSPD can lead to bend-induced cracking of bars with a higher frequency of crack formation for bend angles above 135°. Hence, there are chances of crack formation in close bends of poor quality QST steel rebars which is significant in seismic applications, as ductility of rebars would be reduced.

(6) Based on the findings of this work, acceptance criteria have been proposed using visual and geometrical analyses. The developed 'TM-Ring test' and proposed acceptance criteria could be used by the technicians at the steel plant and construction sites to assess the quality in terms of CSPD.

Declaration of Competing Interest

The authors declare that they have no known competing financial interests or personal relationships that could have appeared to influence the work reported in this paper.

Data availability

The data that has been used is confidential.

Acknowledgements

References

[1] P. Simon, M. Economopoulos, P. Nilles, TEMPCORE, an economical process for the production of high quality rebars, Metallurgical Plant Technology 84 (3) (1984) 80–93.

[2] W.L. Gamble, Thermex-processed reinforcing bars, accessed May 23, 2022, American Concrete Institute 25 (7) (2003) 85–88, https://trid.trb.org/view.aspx?id=662394.

[3] Kuz'menko A.G., Chernenko V.T., Sukharev N.S., Kleshchenko D.A.,, Thermomechanical strengthening of Thermtime rebar, Steel Transl. 46 (2016) 282–284, https://doi.org/10.3103/S0967091216040045.

[4] Nair S.A.O., Gokul P.R., Sethuraj R., Sarvani N., Pillai R.G. (2015). Variations in microstructure and mechanical properties of thermo-mechanically treated (TMT) steel reinforcement bars. In proceedings to a conference - cited fromhttps://www.researchgate.net/publication/324562281 (assessed on 12th September, 2019).

[5] M. Rocha, E. Brühwiler, A. Nussbaumer, Geometrical and Material Characterization of Quenched and Self-Tempered Steel Reinforcement Bars, J. Mater. Civ. Eng. 28 (6) (2016) 04016012, https://doi.org/10.1061/(ASCE)MT.1943-5533.0001355.

[6] S.A.O. Nair, R.G. Pillai, 'TM-ring test' - A quality control test for TMT (or QST) steel reinforcing bars used in reinforced concrete systems, Indian Concr, Inst. J. 18 (2017) 27–35.

[7] E. Candoni, M. Dotta, D. Forni, N. Tesio, C. Albertini, Mechanical behaviour of quenched and self-tempered reinforcing steel in tension under high strain ratio, Mater. Des. 49 (2013) 657–666.

[8] L.P. Kabir, M.A. Islam, Hardened case properties and tensile behaviours of TMT steel bars, Am. J. Mech. Eng. 2 (1) (2014) 8–14.

[9] J. Nikolaou, G.D. Papadimitriou, Microstructures and mechanical properties after heating of reinforcing 500 MPa class weldable steels produced by various processes (Tempcore, microalloyed with vanadium and work-hardened), Constr. Build. Mater. 18 (4) (2004) 243–254, https://doi.org/10.1016/j.conbuildmat.2004.01.001.

[10] G. Rehm, D. Russwurm, Assessment of Concrete Reinforcing Bars made by Tempcore Process, Betonwers Fert.-Tech. 6 (1977) 300–307.

[11] A. Ray, D. Mukerjee, S.K. Sen, A. Bhattacharya, S.K. Dhua, M.S. Prasad, N. Banerjee, A.M. Popli, A.K. Sahu, Microstructure and properties of thermomechanically strengthened reinforcement bars: a comparative assessment of plain-carbon and low-alloy steel grades, J. of Materi. Eng and Perform. 6 (1997) 335–343, https://doi.org/10.1007/s11665-997-0098-9.

[12] S.K. Paul, P.K. Rana, D. Das, S. Chandra, S. Kundu, High and low cycle fatigue performance comparison between micro-alloyed and TMT rebar, Constr. Build. Mater. 54 (15) (2014) 170–179, https://doi.org/10.1016/j.conbuildmat.2013.12.061.

[13] P.C. Basu, P. Shylamoni, A.D. Roshan, Characterisation of steel reinforcement for RC structures: an overview and related issues, Indian Concrete Journal 78 (1) (2004) 19–30.

[14] ASTM-E8, Tensile testing of metals, Am. Soc. Test. Mater. Phila. USA. i (2008) 1–25. 10.1520.

[15] As, nzs,, 4671, Steel reinforcing materials, Standards Association of New Zealand, New Zealand (2001).

[16] ASTM A913 / A913M-15, Standard Specification for High-Strength Low-Alloy Steel Shapes of Structural Quality, Produced by Quenching and Self-Tempering Process (QST), American Society of Testing and Materials, West Conshohocken, PA, 2015.

[17] Astm : a706, a706m -14,, Standard specification for deformed and plain low-alloy steel bars for concrete reinforcement, American Society of Testing and Materials, USA, 2014, p. 2014.

[18] Bs,, 4449, Steel for the reinforcement of concrete – Weldable reinforcing steel – Bar, coil and decoiled product – Specification, British Standard (2005).

[19] IS 1786, High strength deformed steel bars and wires for concrete reinforcement – specification, fourth revision, Bureau of Indian Standards, New Delhi, India, 2008.

[20] IS 13920, Ductile design and detailing of reinforced concrete structures subjected to seismic forces – code of practice, Bureau of Indian Standards, New Delhi, India, 2014.

[21] Jis, G3112, Steel bars for concrete reinforcement, Japanese Standards Association (2004).

[22] Din, 488–1, Reinforcing steels – Part 1: Grades, properties, marking, German National Standard (2009).

[23] IS 1599, Method for bend test, second revision, Bureau of Indian Standards, New Delhi, India, 2012.

[24] F. Djavanroodi, A. Salman, Variability of Mechanical Properties and Weight for Reinforcing Bar Produced in Saudi Arabia, IOP Conference Series, Materials Science and Engineering 230 (1) (2017), 012002, https://doi.org/10.1088/1757-899X/230/1/012002.

[25] S.A.O. Nair, R.G. Pillai, Microstructural and corrosion characteristics of Quenched and Self-Tempered (QST) steel reinforcing bars, Constr. Build. Mater. 231 (2020), 117109, https://doi.org/10.1016/j.conbuildmat.2019.117109.

[26] R.K. Markan, Steel Reinforcement for India, Relev. Quenching Tempering Technol. Steelworld. (2005) 4–9.

[27] D.A. Jones, D. Greene, Electrochemical detection of localized corrosion, Corrosion 25 (9) (1969).

[28] D.A. Jones, Localized Surface Plasticity During Stress Corrosion Cracking, Corrosion 52 (05) (1996).